Azodioxide Radical Cations

Melinda L. Greer, Haripada Sarker, Maria E. Mendicino, and Silas C. Blackstock*

Contribution from the Department of Chemistry, Vanderbilt University, Nashville, Tennessee 37235

Received November 9, 1994. Revised Manuscript Received July 7, 1995[⊗]

Abstract: This report provides the first examples of solution-stable azodioxide radical cations and describes their direct spectroscopic observation and, in one case, their thermal chemistry. The formal oxidation potentials, $E^{o\prime}$, for *N,N'*-dioxo-2,3-diazabicyclo[2.2.2]oct-2-ene (**3**), *N,N'*-dioxo-2,3-diazabicyclo[2.2.1]hept-2-ene (**4**), and *N,N'*-dioxo-1,1'-azobis(norbornane) (**5**) are 1.65, 1.68, and 1.54 V vs SCE, respectively. ESR spectroscopy shows the intermediate cations to be π radicals. Radical cation $\mathbf{5}^{\bullet+}$ (red, λ_m 510 nm) has a five-line ESR spectrum of a(2N) 1.1 G, while $\mathbf{3}^{\bullet+}$ (bronze) has a nine-line ESR spectrum simulated as a(4H) 0.86 and a(2N) 1.22 G. Both $\mathbf{3}^{\bullet+}$ and $\mathbf{5}^{\bullet+}$ decay in seconds to minutes at room temperature. Thermal decomposition of $\mathbf{5}^{\bullet+}$ results in C,N and N,N bond cleavage, yielding 1-norbornyl cation (trapped by solvent) and NO^+ (trapped in low yield by the oxidant under chemical oxidation conditions). Two viable mechanisms are presented for $\mathbf{5}^{\bullet+}$'s thermal decay, both of which invoke nitrosoalkane monomer **5m** as an intermediate. In a related study, oxidation of nitrosoalkane **2m** is found to mediate its facile denitrosation. This work affords the first examples of electron-transfer-mediated C,N bond cleavage of azodioxides and of nitrosoalkanes. Substantial bond weakening is shown to accompany electron loss from these substrates. For **5**, π oxidation leads ultimately to σ C,N bond activation.

Introduction

Removing an electron from an organic molecule influences its molecular structure and dynamics, often dramatically. This is the basis for redox mediation of molecular reactivity, an important developing area of organic chemistry.[1−4] One theme of organic redox chemistry is selective bond activation. Here, we report electron-transfer-mediated C,N bond activation in azoalkane dioxides and in nitrosoalkanes and report the first direct observation of metastable solution-phase azodioxide radical cations.

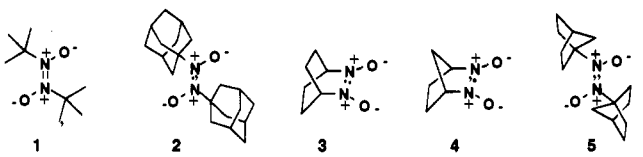

1 **2** **3** **4** **5**

Compounds **1**−**5** are employed as substrates. These structures are selected because their neutral forms are not susceptible to irreversible thermal conversion to oximes, a reaction typical of many azodioxides. Such isomerization occurs via azodioxide monomerization to nitrosoalkanes (eq 1a) which subsequently undergo 1,3 hydrogen migration to form oximes (eq 1b). This

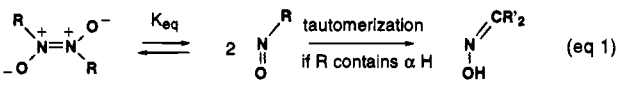

(eq 1a) (eq 1b) (eq 1)

pathway presents a complication which we wish to avoid in our present studies. For azodioxides **1**−**5**, oxime formation is precluded because either (a) the monomeric nitrosoalkanes contain no hydrogen α to nitrogen for migration (as in **1**, **2**, and **5**) or (b) the azodioxides do not monomerize (as in **3** and **4**) (*vide infra*).

Equation 1a shows the azodioxide−nitrosoalkane equilibrium. This equilibrium is dynamic at room temperature in solution but not especially facile.[5,6] In principle, the eq 1a process makes it difficult to study either structural form, monomer or dimer, individually. However, in practice, it is usually possible to control which species predominates in solution. In the solid state, azodioxides exist exclusively in dimeric form (as azodioxides), but in solution at equilibrium, they become predominately monomeric if the alkyl substituent at nitrogen is large. For example, azodioxide **1** is a colorless solid but gives deep blue solutions indicative of substantial monomer formation after dissolution. The pronounced color difference between the monomer (blue) and dimer (colorless) allows easy visual assessment of the presence (or absence) of any monomeric material. Because the rate of approach to equilibrium in solution is moderately slow (30−60 min) at room temperature and very slow at low temperature, it is possible to prepare and maintain nonequilibrium solutions of pure dimer. Conversely, azodioxides with large alkyl groups give dilute solutions of nearly pure monomer at equilibrium. Thus, solutions of either structural form are independently attainable for many azodioxides, allowing investigation of one in the absence of the other. Here, we focus on the chemistry of the dimeric azodioxides **1**−**5** but also present results from a cursory study of the one-electron oxidation chemistry of the monomeric form of **2**, **2m** (1-nitrosoadamantane).

Results

Synthesis of Neutral Azodioxides. Scheme 1 summarizes the synthesis of azodioxides **1**−**5**. Compounds **1**,[7] **2**,[8] and **5** are prepared by amine oxygenation with *m*CPBA to give the corresponding nitrosoalkanes which, upon dimerization, give the azodioxides as solids in moderate to good yield. Compound

[⊗] Abstract published in *Advance ACS Abstracts*, October 1, 1995.

(1) *Photoinduced Electron Transfer*; Fox, M. A., Chanon, A., Ed.; Elsevier: Amsterdam, 1988.
(2) Kochi, J. K. In *Comprehensive Organic Synthesis*; Trost, B. M., Ed.; Pergamon Press: Oxford, 1991; Vol. 7, p 849.
(3) *Advances in Electron Transfer Chemistry*; Mariano, P. S., Ed.; JAI Press: Greenwich, CT, 1991−1993; Vols. 1−3.
(4) Roth, H. D. In *Topics in Current Chemistry*; Mattay, J., Ed.; Springer-Verlag: Berlin, 1992; Vol. 163, p 131.
(5) Snyder, J. P.; Heyman, M. L.; Suciu, E. N. *J. Org. Chem.* **1975**, *40*, 1395−1404.
(6) Greene, F. D.; Gilbert, K. E. *J. Org. Chem.* **1975**, *40*, 1409−1415.
(7) Stowell, J. C. *J. Org. Chem.* **1971**, *36*, 3055−3056.
(8) Forrest, D.; Gowenlock, B. G.; Pfab, J. *J. Chem. Soc., Perkin Trans. 2* **1979**, 576−580.

0002-7863/95/1517-10460$09.00/0

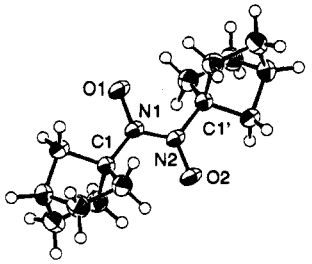

Figure 1. ORTEP plot for X-ray crystal structure of **5** (50% thermal ellipsoids).

Scheme 1

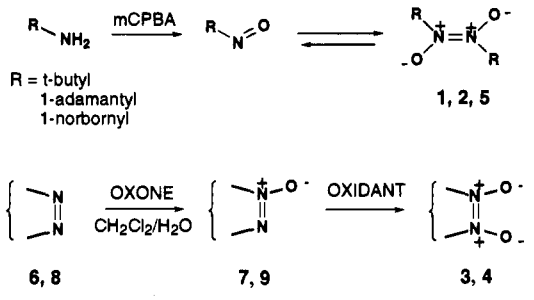

3[5,9] is conveniently prepared by sequential oxygenation of the corresponding azo **6** by oxone,[10] generating azooxide **7** as an observed (and isolable) intermediate. Compound 4[5,9] is best prepared by direct dioxygenation of the corresponding azo **8** using 2 mol equiv of trifluoroperacetic acid. Alternatively, monooxygenation of azo **8** by oxone yields monooxide **9**, which does not react further with oxone under our conditions but can be converted to **4** by treatment with trifluoroperacetic acid.

X-ray Crystal Structure. Crystals of **5** with the morphology of crossed plates grow from cold CH_2Cl_2/Et_2O mixtures. A cut section of these thick plates has been subjected to X-ray diffraction structure analysis. The crystal lattice possesses a monoclinic unit cell ($C_{2/m}$), and solution and refinement of the diffraction data yield a structure (R 0.036, R_w 0.038) whose ORTEP diagram is given in Figure 1. Selected structure parameters are listed in Table 1.

Table 1. Selected Distances and Angles for **5**

	Distances (Å)		
O1–N1	1.269(4)	O2–N2	1.269(4)
N1–N2	1.308(6)	N2–C1′	1.483(5)
N1–C1	1.483(5)		
	Angles (deg)		
O1–N1–N2	120.1(4)	O1–N1–C1	120.7(3)
N2–N1–C1	119.2(4)	O1–N1–N2–O2	180
O1–N1–N2–C1′	0	C1–N1–N2–C1′	180

Table 2. Thermodynamics for Azodioxide Monomerization (Eq 1a)

azodioxide	solvent	T, °C	K_{eq}	$\Delta G°$ [a]	$\Delta H°$ [a]	$\Delta S°$, eu	ref
1	CCl_4	27	2.8	−0.61	12	42	7
2	$CDCl_3$	25	1.9	−0.38			*b*
5	toluene-d_8	25	.00071	4.3	18	46	*b,c*

[a] kcal mol^{-1}. [b] This work. [c] Extrapolated to 25 °C (see the Experimental Section).

Monomer–Dimer Equilibria. When azodioxides **1** and **2** are dissolved in CH_2Cl_2 or CH_3CN, the solutions slowly turn blue as the monomer–dimer equilibrium (eq 1a) is established. In contrast, compounds **3** and **4** do not undergo coloration upon dissolution and compound **5** does so only very slightly. Table 2 gives measured K_{eq} values (monomerization) for compounds **1**, **2**, and **5** as determined by ^{1}H NMR integration of equilibrated mixtures of known concentration. From the temperature dependence of K_{eq} for **5**, we find $\Delta H°$ = 18 kcal/mol and $\Delta S°$ = 46 cal/mol deg for monomerization.

Cyclic Voltammetry. The oxidative cyclic voltammetry (CV) response of azodioxides **1**–**5** is shown in Figure 2.

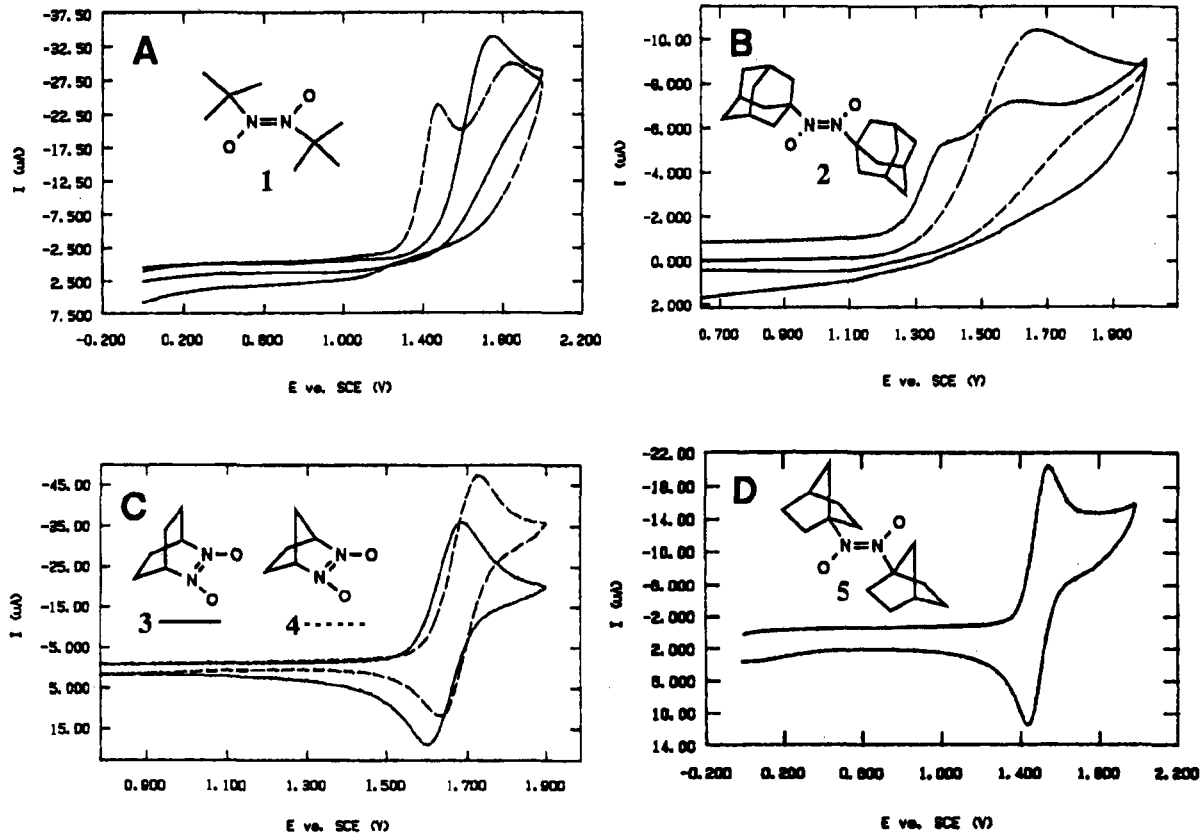

Figure 2. CV traces in acetonitrile (0.1 M tetrabutylammonium perchlorate) for (A) **1** immediately after dissolution (dashed) and after 1 h at room temperature (solid); (B) **2** immediately after dissolution (solid) and after 1 h at room temperature (dashed); (C) **3** (solid) and **4** (dashed); (D) **5**.

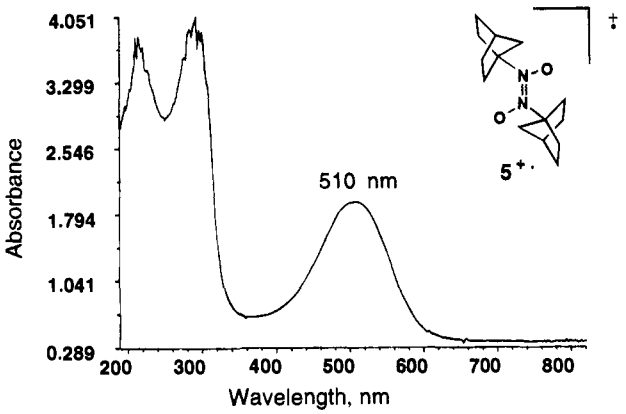

Figure 3. UV−vis spectrum of electrolyzed **5** in acetonitrile at −35 °C.

Table 3. Electrochemical Oxidation Potentials ($E^{o\prime}$)[a] and Peak Potentials (E_{pa})[a] for Azodioxides

substrate	$E^{o\prime}$ [E_{pp}, mV]	E_{pa}
1 (**1m**)		1.47 (1.84)
2 (**2m**)		1.40 (1.59)
3	1.65 [80]	1.69
4	1.68 [92]	1.73
5 (**5m**)	1.54 [117]	1.60 (1.84)

[a] In V vs SCE in CH_3CN at a planar Pt electrode at 200 mV/s scan rate.

Electrochemical oxidation of **1** has been previously studied by the groups of Blount[11] and of Tordo,[12] who found that $\mathbf{1}^{\bullet+}$ is too short-lived to afford chemically reversible cyclic voltammograms. In agreement with their work, we also find that anodic oxidation of **1** by CV shows two chemically irreversible waves, $E_{pa}(1) = 1.47$ and $E_{pa}(2) = 1.84$ V vs SCE. These peaks are assigned as the one-electron oxidations of dimer **1** and monomer **1m** (*t*-BuNO), respectively.[11,12] Two waves are observed only if the CV trace is recorded shortly after dissolution of **1** in the electrolyte medium. At longer times, only the higher potential peak is observed which reflects oxidation of the monomer **1m**, present in large excess over dimer **1** at equilibrium. As previously observed,[12] even under cold conditions just after dissolution of **1**, the CV trace shows a small component of the second (monomer) oxidation wave. This result led Tordo and co-workers to postulate that monomeric *t*-BuNO is produced from $\mathbf{1}^{\bullet+}$ under the CV conditions.

Azodioxide **2** gives a CV portrait very similar to that observed for **1** but shifted to slightly lower potentials. Both $\mathbf{2}^{\bullet+}$ and $\mathbf{2m}^{\bullet+}$ have solution lifetimes less than milliseconds at room temperature as indicated by the chemically irreversible nature of the oxidation waves. Analogous to **1**'s anodic oxidation dynamics, it appears that monomer **2m** forms from $\mathbf{2}^{\bullet+}$ under CV conditions because the second oxidation wave is always observed, even from colorless solutions of **2** at low temperatures which must contain very little **2m**. The CV-derived anodic peak potentials for **1** and **2** (and for **1m** and **2m**) are listed in Table 3.

In contrast to the short solution lifetimes of $\mathbf{1}^{\bullet+}$ and $\mathbf{2}^{\bullet+}$, we observe long lifetimes (of at least seconds) for radical cations derived from **3**, **4**, and **5** as indicated by their chemically reversible CV waves (Figure 2). The formal oxidation potentials ($E^{o\prime}$ values) for these azodioxides range from 1.5 to 1.7 V vs SCE (Table 3). At scan rates of <200 mV/s, the cyclic voltammogram of **4** becomes chemically quasi-reversible, indicating that $\mathbf{4}^{\bullet+}$'s lifetime under these conditions is only on the order of seconds. Both **3** and **5** give fully chemically reversible cyclic voltammograms at scan rates as low as 20 mV/s, and their radical cations are thus longer-lived than $\mathbf{4}^{\bullet+}$. The CV traces for all three azodioxides **3**−**5** are insensitive to saturation of the solvent with oxygen.

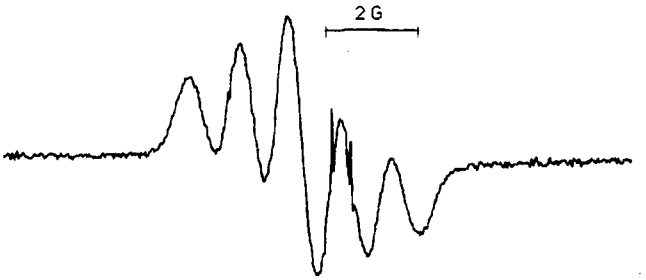

Figure 4. ESR spectra of $\mathbf{5}^{\bullet+}$ in CH_3CN at −35 °C.

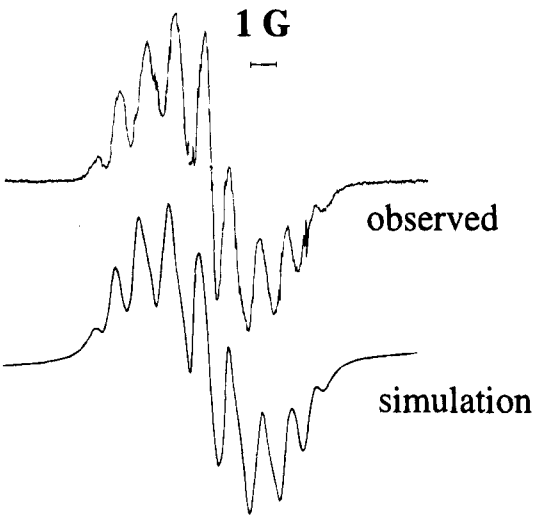

Figure 5. ESR spectrum of $\mathbf{3}^{\bullet+}$ in CH_3CN at −35 °C and simulation (see text).

The long solution lifetimes of $\mathbf{3}^{\bullet+}$ and $\mathbf{5}^{\bullet+}$ allow direct spectroscopic characterization of these reactive intermediates. Because of the relatively high oxidation potentials of these substrates, they are more easily generated quantitatively by low-temperature bulk electrolysis than by chemical oxidation. Cold solutions of electrogenerated $\mathbf{3}^{\bullet+}$ and $\mathbf{5}^{\bullet+}$ are analyzed spectroscopically as described below.

Optical and ESR Spectroscopy of $\mathbf{3}^{\bullet+}$ and $\mathbf{5}^{\bullet+}$. Bulk electrolysis of **5** in cold (−35 °C) acetonitrile at a Pt foil electrode generates a red solution which shows a UV−vis absorption peak with λ_m 510 nm ($\epsilon \sim 800$)[13] (Figure 3) which we assign to the radical cation $\mathbf{5}^{\bullet+}$. The red color bleaches in seconds upon warming to 25 °C but persists for hours at −35 °C. Cold electrolysis of **3** in acetonitrile generates a bronze solution whose color bleaches in minutes when the solution is warmed to room temperature.

The colored electrolysis solutions of $\mathbf{5}^{\bullet+}$ and $\mathbf{3}^{\bullet+}$ are ESR active (see Figures 4 and 5, respectively). The red solution of $\mathbf{5}^{\bullet+}$ shows a five-line ESR spectrum with a line separation of ~1.1 G, while the bronze solution of $\mathbf{3}^{\bullet+}$ displays a nine-line pattern, also with a line separation of roughly 1 G. The latter spectrum is simulated using a(2N) 1.22 G, a(4H) 0.86 G, and

(9) Singh, P. *J. Org. Chem.* **1975**, *40*, 1405−1408.
(10) du Pont tradename for monopersulfate compound, $2KHSO_5$−$KHSO_4$−K_2SO_4.
(11) McIntire, G. L.; Blount, H. N.; Stronks, H. J.; Shetty, R. V.; Janzen, E. G. *J. Phys. Chem.* **1980**, *84*, 916−921.
(12) Gronchi, G.; Courbis, P.; Tordo, P.; Mousset, G.; Simonet, J. *J. Phys. Chem.* **1983**, *87*, 1343−1349.
(13) The concentration of electrogenerated radical cation is measured by controlled potential coulometry. The resulting ϵ value should be regarded as a lower limit because some decomposition of $\mathbf{5}^{\bullet+}$ during sample handling is probable.

Table 4. Oxidation of 1-Nitrosoadamantane (**2m**) by $Ar_3N^{\bullet+}SbCl_6^-$

	Reactants[a]			Products[a]		
run	**2m**[b]	Ar_3N^+	**12**[c]	**2m**	**13**	AdOH
1	1	1	0		0.87	0.14
2	1	0.5	0		0.85	0.14
3	1	0.5	3	0.75	0.25	

[a] Amounts listed as molar equivalents relative to [**2m**]. [b] 25 mL of 20.2 mM **2m** in CH_3CN. [c] 2,6-Di-*tert*-butyl-4-methylpyridine.

a line width of 0.48 G (Figure 5). These spectra were recorded at −35 °C, at which temperature the ESR signals persist for hours.

Thermal Chemistry of Azodioxide 5$^{\bullet+}$. At 3 °C in acetonitrile, the 510 nm band of **5**$^{\bullet+}$ decays by first-order kinetics with $k = (7.9 \pm 1.0) \times 10^{-3}$ s^{-1}. Product analysis of the bleached red solution after hydrolytic workup shows 1-norbornylacetamide (**10**) and starting azodioxide **5** as the major products. Chemical oxidation of **5** with 1 mol equiv of tris(2,4-dibromophenyl)aminium hexachloroantimonate ($Ar_3N^{\bullet+}SbCl_6^-$) in acetonitrile at 25 °C results, after basic hydrolytic workup, in a 20−25% yield of acetamide **10** along with recovered **5** and reduced oxidant (Ar_3N) as determined by quantitative ^{1}H NMR and GC/MS analyses (eq 2). In addition

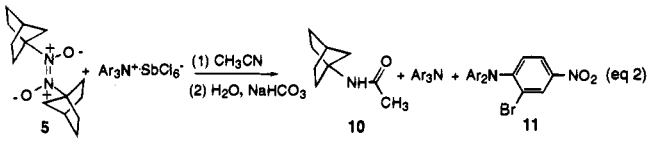

to reduced oxidant Ar_3N, an aromatic byproduct is formed in about ~9% yield (based on starting $Ar_3N^{\bullet+}$). Isolation and spectroscopic characterization of this byproduct show it to be bis(2,4-dibromophenyl)(2-bromo-4-nitrophenyl)amine (**11**). The Ar_3N:**11** ratio is about 10 from a 1:1 **5**:$Ar_3N^{\bullet+}$ reaction as deduced by NMR of the crude reaction mixture. Amine **11** can be independently synthesized by reaction of $Ar_3N^{\bullet+}SbCl_6^-$ with equimolar $NOPF_6$ or NO_2PF_6 in roughly 13 and 45% yields, respectively. Interestingly, the corresponding reaction between NO^+ (or NO_2^+) and neutral Ar_3N (1:1) is not as efficient, giving <1% of **11**.[14]

Nitrosoalkane Oxidation. Because nitrosoalkanes are potential intermediates in the thermal reaction of azodioxide radical cations (*vide infra*), we have conducted a preliminary study of nitrosoalkane reactivity under oxidative conditions, the results of which are described here. Chemical oxidation of 1-nitrosoadamantane (**2m**) in CH_3CN by $Ar_3N^{\bullet+}SbCl_6^-$ yields C,N bond cleavage products (eq 3, Table 4). In the absence of any

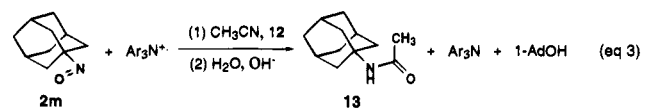

added base, nitrosoalkane **2m** decays completely, even when only 0.5 mol equiv of oxidant is used (run 2, Table 4). We suspect that trace acid generated from the electron-transfer (ET) reaction may catalyze **2m** decomposition. Indeed, we find that **2m** undergoes acid-catalyzed decomposition by $HBF_4 \cdot OEt_2$. To preclude acid-derived chemistry, 2,6-di-*tert*-butyl-4-methylpyridine (**12**) is added to the reaction mixture. In the presence of base **12**, **2m** reacts exclusively by an ET mechanism and 1 mol of **2m** requires 2 mol of oxidant (run 3, Table 4) for complete reaction. The net reaction upon electron removal from **2m** is denitrosation. Careful analysis of the crude reaction mixture by ^{1}H NMR shows that a trace of aromatic amine **11** is formed in the **2m** reaction with $Ar_3N^{\bullet+}$.[15]

Discussion

Monomer−Dimer Equilibria for Azoalkane Dioxides. The bicyclic azodioxides **3** and **4** do not monomerize in solution because of geometrical constraints imposed by the bicyclic framework which impede the formation of the preferred transition state geometry for N,N bond cleavage. Woodward and Hoffmann[16,17] first suggested and Greene and Gilbert[6] later confirmed that the allowed nitrosoalkane dimerization/azodioxide monomerization pathway is not a least motion one, but rather requires the nitroso groups to interact in mutually perpendicular planes at the transition state to optimize HOMO−LUMO interactions in a fashion analogous to that which occurs along the "allowed" singlet methylene dimerization pathway. Azodioxides **3** and **4** are unable to achieve this transition state geometry easily and therefore do not readily equilibrate with their nitrosoalkane "monomeric" forms in solution. It is also true that **3** and **4** lack the full entropic gain of N,N bond breaking afforded other azodioxide structures such as **1**, **2**, or **5** because of the cyclic nature of the azodioxide linkage in the former. Structures **1**, **2**, and **5** are unconstrained and freely interconvert between monomer and dimer forms whose relative population at equilibrium is determined by thermodynamics.

Generally, nitrosoalkane dimer structures are enthalpically preferred (but entropically disfavored) relative to the monomer structures. Steric strain in the dimer when substituents at nitrogen are large results in less of an enthalpic advantage for the dimer than when substituents are small, and this leads to an equilibrium constant which usually favors the monomer for hindered azodioxides such as **1** and **2** (see Table 2). Interestingly, the 1-norbornyl groups of **5** are, although tertiary, substantially less sterically demanding than the *tert*-butyl groups of **1** or the 1-adamantyl groups of **2** as judged by relative K_{eq} values for monomerization of the azodioxides. Apparently, the 1-norbornyl alkyl group is sufficiently "tied back" to render it sterically smaller than unconstrained tertiary alkyl groups. In any event, **5** is a unique tertiary-substituted noncyclic azoalkane dioxide, one with a thermodynamic preference for the dimer at room temperature in solution, making its dimer chemistry especially convenient to study.

One-Electron Oxidation. Although azodioxides are formally oxidized derivatives of azoalkanes, they are not substantially more difficult to remove electrons from than are azoalkanes because azodioxides contain an electron-rich π system (isoelectronic with 1,3-butadiene dianion) with a π^* HOMO. One would thus expect to generate π radical cations from azodioxides, in contrast to the σ radical cations formed from azoalkanes.[18] From CV data for 1,1′-azobis(norbornane)[18,19] and its *N*,*N*′-dioxide (**5**), we find that dioxygenation increases the formal oxidation potential by only 0.14 V in this case.[20]

UV−Vis and ESR Spectroscopy. We assign the 510 nm optical transition of **5**$^{\bullet+}$ to an n → π^* electronic excitation. A calculational estimate of the excitation energy for n → π^*

(14) The reactive intermediates which lead to nitration product **11** are not yet known. Formation of **11** appears to derive from NO^+ reaction with $Ar_3N^{\bullet+}$ or perhaps from NO radical reaction with $Ar_3N^{\bullet+}$. The latter reactant pair can also undergo exothermic ET to NO^+ and neutral Ar_3N whose further reaction is not efficient in producing nitration product **11** (see text).

(15) The reaction of NO^+ with $Ar_3N^{\bullet+}$ is rather slow. In the oxidation of **2m** by $Ar_3N^{\bullet+}$, NO^+ generation and oxidant consumption are both rapid which we suggest minimizes their reaction time and leads to only trace formation of byproduct **11**.

(16) Hoffmann, R.; Gleiter, R.; Mallory, F. *J. Am. Chem. Soc.* **1970**, *92*, 1460−1466.

(17) Hoffmann, R.; Woodward, R. B. *Science* **1970**, *167*, 825−831.

(18) Mendicino, M. E.; Blackstock, S. C. *J. Am. Chem. Soc.* **1991**, *113*, 713−715.

(19) $E^{\circ\prime}$ for 1,1′-azobis(norbornane) is 1.40 V vs SCE in CH_3CN (0.1 M Bu_4NClO_4).

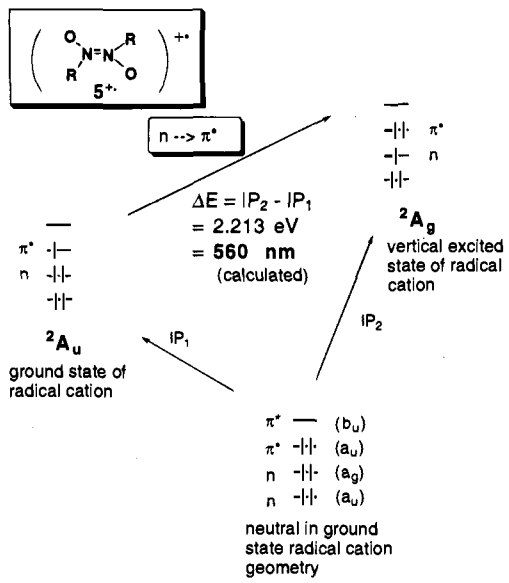

Figure 6. Calculated optical transition energies by AM1 using Koopmans' theorem.

excitation in $5^{\bullet+}$ is obtained using AM1/RHF[21] calculations by equating ΔE for the transition to the calculated n and π^* orbital energy difference in a hypothetical molecule **5** held in $5^{\bullet+}$'s geometry (as optimized by AM1/UHF) in accord with Koopmans' theorem.[22] Figure 6 shows the method diagramatically.[23] This treatment predicts an absorption maximum for $5^{\bullet+}$ ($n \rightarrow \pi^*$) at 560 nm, within 5 kcal/mol of the observed absorption at 510 nm. Whether this method will be generally useful for calculating the UV−vis transitions of azodioxide radical cations remains to be demonstrated, but it works moderately well in this instance.

The ESR spectra for $3^{\bullet+}$ and $5^{\bullet+}$ are the first such spectra recorded in solution for azodioxide radical cations. For $3^{\bullet+}$, the nine-line pattern is thought to arise from a(2N) and a(4H) splittings as simulated. The H splittings are postulated to derive from the set of exo H's on the ethylene bridges by long-range back orbital overlap with the ONNO π system. For $5^{\bullet+}$, the spectrum is assigned as a(2N) 1.1 G.

Symons and co-workers[24] have previously observed an anisotropic ESR spectrum assigned to $1^{\bullet+}$ in the solid state. This species was generated by freon matrix γ-ray oxidation of a mixture of **1** and **1m**. The spectrum showed a single five-line pattern, assigned as a_x(2N) 5.0 G. The projected a_{iso}(2N) value would thus be 1.7 G under rotationally averaged conditions. Our ESR data for $3^{\bullet+}$ and $5^{\bullet+}$, for which a(2N) values of 1.1−1.2 G are observed, are in general agreement with Symons' anisotropic data for $1^{\bullet+}$.

The small isotropic nitrogen splittings for $5^{\bullet+}$ and $3^{\bullet+}$ support the assignment of these species as π radicals. The odd electron spin density in the ONNO π system of these radical cations appears to be mostly on the terminal oxygen atoms as expected for a butadiene-like π_3 SOMO. Assuming the magnitude of the nitrogen splitting scales linearly with the π electron density of the unpaired spin at nitrogen for planar nitrogens, one may estimate the π spin density at each nitrogen in $5^{\bullet+}$ (or in $3^{\bullet+}$) by comparison to the a(2N) value of 11 G for hydrazine radical cation[25] which is thought to be planar or very nearly so and which may be assumed to have 0.5 spin at each nitrogen. Such qualitative analysis suggests that the π spin density at nitrogen in $5^{\bullet+}$ is ~0.05, leaving ~0.45 π spin density on each of the oxygens. AM1/UHF[21] calculation of $5^{\bullet+}$ gives the odd electron π spin density to be 0.035 at nitrogen and 0.468 at oxygen. These numbers are not too far from those for π_3* of 1,3-butadiene as predicted by Hückel theory (0.14 at the internal positions and 0.36 at the terminal carbons). We conclude that the ESR spectra of $5^{\bullet+}$ and $3^{\bullet+}$ support their assignments as π radicals with most of the spin density on oxygen.

Scheme 2

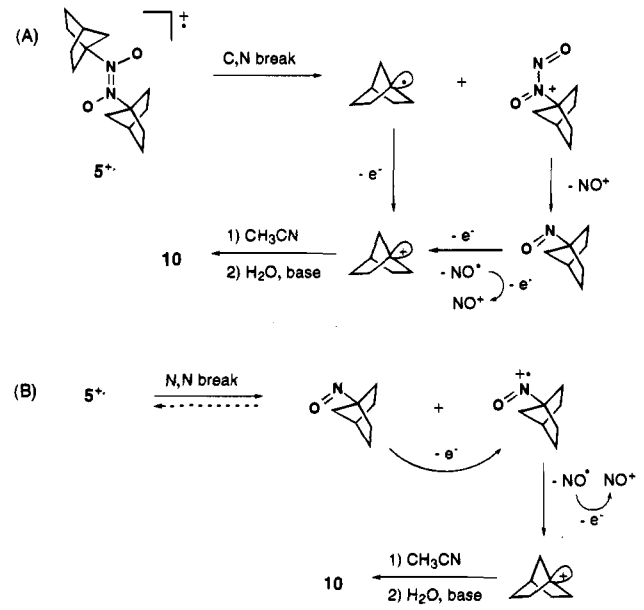

Thermal Chemistry of Azodioxide Radical Cation $5^{\bullet+}$. The $5^{\bullet+}$ lifetime is hours at −35 °C but only seconds at ambient temperature. In acetonitrile, $5^{\bullet+}$ thermal decay is first order, and the major norbornyl-containing product after hydrolytic workup of the reaction is *N*-1-norbornylacetamide (**10**) (eq 2). Scheme 2 gives two plausible mechanistic postulates for the transformation.[26] From the product structure, it is clear that rather facile C,N bond breaking in $5^{\bullet+}$ occurs at some stage under the oxidative conditions. In view of amine **11** formation (which implies the generation of free NO^+ or an NO^+ "reagent" under the reaction conditions), it appears likely that N,N cleavage also occurs, but the order of these events remains unknown at present.

Both mechanistic postulates of Scheme 2 invoke monomeric nitrosoalkane intermediates, consistent with their implied formation from the CV behavior of **1** and of **2**. A control experiment in which **5** (2 mM in CH_3CN) is heated to 80 °C to generate an observable population of monomer **5m** (λ_m = 680 nm) and then quickly cooled to 0 °C and observed by UV−vis spectroscopy shows that **5m** does not decay (dimerize) fast at 0 °C. Thus, if formed in the $5^{\bullet+}$ thermal reaction at 0 °C, **5m** would be observable at ≥0.01 mM concentrations. Therefore, we must

(20) When **3** and its corresponding azo compound are placed on a plot of IP_v vs $E^{o\prime}$ (see reference) containing various π oxidizable substrates, the azo compound is much farther from the "no relaxation" line[18] (18.4 kcal/mol) than is **3** (~6 kcal/mol), indicating that the azo has a much larger reorganization energy upon electron loss than does **3**. This is consistent with π oxidation of the ONNO linkage. Nelsen, S. F.; Blackstock, S. C.; Petillo, P. A.; Agmon, I.; Kaftory, M. *J. Am. Chem. Soc.* **1987**, *109*, 5724−5731.

(21) Dewar, M. J. S.; Zoebisch, E. G.; Healy, E. F.; Stewart, J. J. P. *J. Am. Chem. Soc.* **1985**, *107*, 3902−3909.

(22) Koopmans, T. *Physica* **1934**, *1*, 104−113.

(23) Haselbach, E.; Bally, T.; Gschwind, R.; Klemm, U.; Lanyiova, Z. *Chimia* **1979**, *33*, 405−411.

(24) Chandra, H.; Keeble, D. J.; Symons, M. C. R. *J. Chem. Soc., Faraday Trans. 1* **1988**, *84*, 609−616.

(25) Adams, J. Q.; Thomas, J. R. *J. Chem. Phys.* **1963**, *39*, 1904.

(26) (a) It is possible that initial C,N cleavage of $5^{\bullet+}$ (as in Scheme 3) gives 1-norbornyl cation and the corresponding nitroxyl-like radical along the 3a fragmentation path. Which oxidation state of the intermediates is preferred is a matter of the relative oxidation potentials of the radicals—values not known presently. (b) Either initial N,N or C,N bond cleavage in azodioxide radical cations is consistent with the observed increased kinetic stability of $3^{\bullet+}$−$5^{\bullet+}$ compared to $1^{\bullet+}$ and $2^{\bullet+}$.

Scheme 3

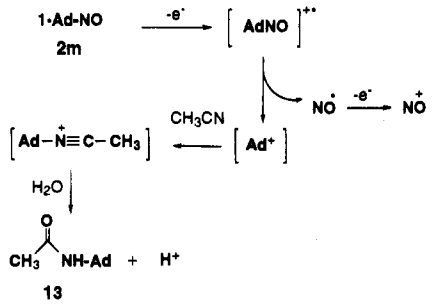

conclude that, if formed, **5m** never builds up to detectable levels under the $5^{\bullet+}$ thermolysis conditions because its optical absorption is not observed during the course of the reaction. If formed from $5^{\bullet+}$, **5m** must rapidly decay, not by dimerization, but more likely by oxidative denitrosation. We expect $\mathbf{5m}^{\bullet+}$ to be extremely short-lived on the basis of our study of $\mathbf{2m}^{\bullet+}$ and theoretical predictions. Chemical oxidation of **2m** shows that $\mathbf{2m}^{\bullet+}$ is prone to facile denitrosation and that the stoichiometry of the reaction requires 2 mol equiv of oxidant. Upon aqueous workup, 1-adamantylacetamide (**13**) is formed. Scheme 3 shows our proposed mechanism for oxidative C,N bond cleavage of **2m**.

Facile C,N bond cleavage in $R-NO^{\bullet+}$ species is expected. Consider 2-nitroso-2-methylpropane as an example. In this case, the C,N bond dissociation energy for the neutral nitrosoalkane is known to be ~40 kcal/mol.[27] Using E_{pa} (anodic peak potential = 1.84 V) for *t*-Bu-NO as an estimate of its unknown $E^{\circ\prime}$ value and using the known $E^{\circ\prime}$ (0.10 V) for oxidation of *t*-Bu radical,[28,29] we estimate C,N bond breaking for $t\text{-BuNO}^{+\bullet}$ to be roughly 39 kcal/mol easier than such for *t*-BuNO. Therefore, we expect the C,N bond in $t\text{-BuNO}^{+\bullet}$ to be extremely weak or nonexistent and predict short lifetimes for $RNO^{+\bullet}$ structures in general, consistent with their possible intermediacy as transient species in azodioxide radical cation thermal decay.[30]

Summary and Conclusions

The first examples of solution-stable azodioxide radical cations are reported. These colored species show n → π* absorption in the visible range and have small ESR *a*(2N) values of ~1 G, indicating that most of the electron spin is on oxygen in these radicals. Thermal decay of $5^{\bullet+}$ gives C,N and N,N bond cleavage. The stoichiometry for oxidative fragmentation of **5** requires at least 4 mol equiv of oxidant to fully consume 1 mol of azodioxide. Alkylnitroso compounds, the monomeric forms of azodioxides, are potential intermediates in the thermal azodioxide radical cation fragmentation reaction. Separate studies on 1-nitrosoadamantane show that this nitrosoalkane radical cation undergoes denitrosative C,N bond breakage. Thus, ET-mediated C,N bond breaking is found for an azodioxide and a nitrosoalkane.

(27) Blatt, L.; Robinson, G. N. *The Chemistry of Amino, Nitroso, and Nitro Compounds and their Derivatives*; Wiley: New York, 1982; pp 1035–1084.

(28) Wayner, D. D. M.; McPhee, D. J.; Griller, D. *J. Am. Chem. Soc.* **1988**, *110*, 132–137.

(29) Wayner, D. D. M.; Parker, V. D. *Acc. Chem. Res.* **1993**, *26*, 287–294.

(30) Since the C,N bond of 1-nitrosonorbomane (**5m**) will no doubt be stronger than that of *t*-BuNO and the oxidation potential of 1-norbornyl radical higher than that of *t*-Bu radical, it is probable that the 1-nitrosonorbomane radical cation will be a bound state with a stronger C,N bond than present in *t*-BuNO radical cation. Nevertheless, C,N bond weakening of 30–40 kcal mol^{-1} is expected for $\mathbf{5m}^{\bullet+}$, which will likely impart kinetic instability to its C,N bond consistent with the chemically irreversible oxidation of **5m** by CV at low temperature and with possible $\mathbf{5m}^{\bullet+}$ intermediacy in **5**'s oxidative decay reaction.

Experimental Section

General Methods. Melting points were taken with a Thomas Hoover apparatus and are uncorrected. C, H, N analyses were obtained from the microanalytical lab, Department of Chemistry, Vanderbilt University, or from Atlantic Microlab Inc., Norcross, GA. IR spectra were obtained from a Perkin Elmer 1600 IR spectrometer using a reference to polystyrene film and UV–vis data from a Hewlett Packard 8452A diode array spectrometer equipped with a temperature-controlled cell compartment. Bruker AC-300 and AM-400 NMR spectrometers were used, and chemical shifts were referenced to residual undeuterated solvent shifts. The ^{13}C NMR carbon multiplicities were determined by DEPT NMR experiments. ESR spectra were taken on a Varian E-112 model V-3900 spectrometer. Routine MS data were recorded on a Hewlett-Packard 5890/5971 GC/MS using a fused silica capillary column (25 m) of cross-linked methylsilicone and operating in EI mode at 70 eV ionizing voltage. An EG&G Princeton Applied Research Potentiostat/Galvanostat Model 273 was used to record electrochemical data. A four-necked CV cell (10 mL) equipped with a Pt disc (1.5 mm diameter) working electrode, a Pt wire counter electrode, and a saturated calomel electrode (SCE) reference was used for routine CV measurements which were carried out under an inert atmosphere. Tetrabutylammonium perchlorate or tetrafluoroborate (TBAP or $TBABF_4$, Kodak) was used as supporting electrolyte (0.1 M solution) for electrochemical experiments. A capacitor (0.1 μF), connected between the reference electrode and counter electrode, was used to reduce background noise. Bulk electrolysis was conducted in a multicomponent cell in which the anodic, cathodic, and reference redox reactions were isolated to separate compartments by fine glass frits.

Acetonitrile (HPLC grade) was refluxed and then distilled over P_2O_5 before use. Cyclohexane and methylene chloride were stirred overnight over concentrated H_2SO_4, decanted and washed with aqueous $NaHCO_3$ and then with water, and finally refluxed and distilled from CaH_2.

***N,N'*-Dioxoazobis(2-methyl-2-propane) (1).** Azodioxide **1** was prepared by *tert*-butylamine oxygenation in a manner analogous to that described in the literature[31] except that *m*CPBA was used as oxidant in place of peracetic acid (mp 70–71 °C).

***N,N'*-Dioxo-1,1'-azobis(adamantane) (2).** Azodioxide **2** has been previously synthesized by dichromate oxidation of *N*-1-adamantylhydroxylamine.[8,32,33] We prepared **2** according to the following variation of the procedure used to prepare **1**. From an addition funnel, a solution of *m*CPBA (70%, 9.12 g, 52.9 mmol) in ethyl acetate (10 mL) was added dropwise over a period of 30 min to a stirring heterogeneous solution of 1-adamantylamine (12.0 g, 80.4 mmol) dissolved in a mixture of ether (150 mL) and water (100 mL) in a 500 mL round-bottomed flask. The reaction mixture turned blue upon addition of the *m*CPBA. After addition, the mixture was stirred for 1 h. The resulting blue solution was periodically tested with starch paper to detect the presence of any unreacted *m*CPBA, and the reaction was continued until all *m*CPBA was consumed. Any excess *m*CPBA was quenched by adding small amounts of adamantylamine until a negative starch test resulted. The reaction mixture was transferred to a separatory funnel, the layers were separated, and the blue organic layer was washed successively with 20% aqueous Na_2CO_3 (3 × 200 mL), 8 N aqueous HCl (3 × 200 mL), and water (3 × 150 mL). The resulting blue solution was dried over anhydrous K_2CO_3, filtered, and evaporated *in vacuo* to give a bluish solid. Pure nitrosoadamantane (1.53 g) was crystallized from ether as a colorless solid (36.6%). Unreacted 1-adamantylamine (8.5 g) was isolated from the aqueous HCl fraction after basification with solid NaOH followed by ether extraction and evaporation. Solid dimer **2** turns blue and sublimes at 150–153 °C (lit.[33] mp 179.5 °C). ^1H NMR (300 MHz, $CDCl_3$) δ 2.35 (br s, 12H), 2.16 (s, 6H), 1.66 (br s, 12H). Nitrosoadamantane monomer (**2m**): UV–vis (chloroform) λ_{max} (nm) (ε) 684 (5.66); ^1H NMR (300 MHz, $CDCl_3$) δ 2.20 (br s, 3H), 1.86 (br s, 6H), 1.76–1.73 (m, 6H); ^{13}C NMR (50 MHz, $CDCl_3$) 36.86 (CH_2), 36.23 (CH_2), 29.89 (C), 28.73 (CH).

***N,N'*-Dioxo-2,3-diazabicyclo[2.2.2]oct-2-ene (3).** 2,3-Diazabicyclo-

(31) Corey, E. J.; Gross, A. W. *Tetrahedron Lett.* **1984**, *25*, 491–494.

(32) Hartgerink, J. W.; Engberts, J. B. F. N.; Wajer, A. J. W.; Boer, T. J. d. *Recl. Trav. Chim.* **1969**, *88*, 481–484.

(33) Stetter, H.; Smulders, E. *Chem. Ber.* **1971**, *104*, 917–923.

[2.2.2]oct-2-ene[34] (200 mg, 1.82 mmol) was dissolved in 2 mL of CH_2Cl_2 and mixed with 3.80 g of oxone ($2KHSO_5 \cdot KHSO_4 \cdot K_2SO_4$, 6.18 mmol) dissolved in a minimal amount of H_2O (~15 mL). The two-phase mixture was vigorously stirred in a flask equipped with a reflux condenser while the mixture was heated to reflux for 7 days. A CH_2Cl_2 aliquot from the mixture showed by GC about a 3:1 mixture of dioxide:monooxide products. The mixture was cooled and the organic layer separated. The aqueous layer was washed with CH_2Cl_2 (5 × 10 mL), and the combined organic extracts were dried over anhydrous K_2CO_3. The solvent was removed *in vacuo* to yield an off-white solid residue which was washed thoroughly with 100 mL of ether and filtered. (Residual *N*-oxo-2,3-diazabicyclo[2.2.2]oct-2-ene can be recovered in nearly pure form from the ether wash.) The resulting ether-insoluble solid was dissolved in a minimal amount of CH_3CN to which a small amount of ether was added, and crystallization was induced at −25 °C. Colorless cubic crystals of **3** resulted (90 mg, 35%): mp (°C) 221−222 (dec) (lit. 221−222 (dec),[5] 236−237 (dec)[9]); ^{1}H NMR (300 MHz, $CDCl_3$) δ 2.02 (br d, 4H), 2.29 (br d, 4H), 4.73 (s, 2H).

***N,N'*-Dioxo-2,3-diazabicyclo[2.2.1]hept-2-ene (4).**[5,9] Azodioxide **4** was prepared by trifluoroperoxyacetic acid oxidation of 2,3-diazabicyclo[2.2.1]hept-2-ene[34] in 56% yield according to a published procedure:[9] mp (°C) 135−137 (dec) (lit. 142−144 (dec);[5] 153−154 (dec)[9]).

1-Norbornanecarboxylic Acid. A suspension of 13.3 g (479 mmol) of lithium dispersion (25% wt/wt) in mineral oil in 100 mL of anhydrous cyclohexane, kept under an argon atmosphere, was heated to reflux in a 2 L three-necked flask, and a solution of 25.28 g (194 mmol) of 1-chlorononorbornane[35] in 100 mL of cyclohexane was added dropwise with stirring via an addition funnel. Stirring and heating were continued for 12 h. The reaction flask was then cooled in an ice bath and diluted with ~500 mL of cyclohexane. The argon stream was replaced by a stream of carbon dioxide (passed through a drying tube containing anhydrous $CaSO_4$ and into the solution). After carbonating for 5 h, the mixture was carefully treated at 0 °C in sequence with isopropyl alcohol (75 mL), ethanol (75 mL), and finally water (50 mL). The resulting two-phase reaction mixture was then acidified with 6 N HCl to pH 3. The aqueous layer was separated and extracted with ether (2 × 100 mL). The combined organic layers were then extracted with 10% NaOH (5 × 100 mL). The resulting aqueous extracts were combined and acidified to pH 2 with concentrated HCl and extracted with ether (3 × 150 mL). The resultant ether solution was dried over anhydrous Na_2SO_4 and evaporated *in vacuo* to yield a pale yellow solid product (14.81 g, 55%): mp 107−110 °C (lit.[35] mp 106−109 °C); ^{1}H NMR (300 MHz, $CDCl_3$) δ 1.32 (m, 2H), 1.59 (m, 2H), 1.70 (m, 2H), 1.90 (m, 2H), 2.31 (s, 1H).

***N,N'*-Dioxo-1,1'-azobis(norbornane) (5).** A solution of *m*CPBA (71%, 9.42 g, 55 mmol) in CH_2Cl_2 (75 mL) was added dropwise to a solution of 1-norbornylamine (prepared from 1-norbornanecarboxylic acid)[36] (3.03 g, 27 mmol) in 1:1 CH_2Cl_2/10% aqueous Na_2CO_3 (300 mL) under argon at 0 °C. The pale blue reaction mixture was stirred at room temperature until starch−iodide paper indicated that there was no *m*CPBA remaining. The organic layer was separated and washed with 10% Na_2CO_3 (3 × 50 mL), 4 N aqueous HCl (3 × 50 mL), and water (2 × 50 mL). The resulting solution was dried over anhydrous K_2CO_3 and evaporated *in vacuo* to give a pale yellow solid (2.63 g, 77%). Compound **5** was purified by sublimation (100 °C, 0.01 mmHg) and column chromatography on silica gel (CH_2Cl_2 eluent) or best by recrystallization from CH_2Cl_2/Et_2O mixtures: mp 157−160 °C (sublimed); IR (KBr, cm^{-1}) 2955, 1458, 1279, 927, 705; ^{1}H NMR (400 MHz, $CDCl_3$) δ 1.50 (m, 2H), 1.80 (m, 4H), 1.95 (s, 2H), 2.20 (s, 1H), 2.35 (m, 2H); ^{13}C NMR (100 MHz, $CDCl_3$) δ 29.58 (CH_2), 29.99 (CH_2), 33.12 (CH), 41.40 (CH_2), 83.58 (C). MS (EI, *m/z*) 125 (11), 95 (71), 67 (100), 55 (55), 41 (45). Anal. Calcd for $C_{14}H_{22}N_2O_2$: C, 67.17; H, 8.86; N, 11.19. Found: C, 67.22; H, 8.85; N, 10.99.

X-ray Crystal Structure of *N,N'*-Dioxo-1,1'-azobis(norbornane) (5). A colorless prism crystal of $C_{14}H_{22}N_2O_2$ having approximate dimensions of 0.10 × 0.25 × 0.40 mm was mounted on a glass fiber. All measurements were made on a Rigaku AFC6S diffractometer with graphite monochromated Mo Kα radiation. Cell constants and an orientation matrix for data collection, obtained from a least-squares refinement using the setting angles of 24 carefully centered reflections in the range $15.93 < 2j < 32.50°$, corresponded to a monoclinic cell with dimensions $a = 6.478(3)$ Å, $b = 10.136(3)$ Å, $c = 9.742(2)$ Å, $\beta = 90.97(3)°$, and $V = 639.6$ (4) Å^3. For $Z = 2$ and F.W. = 250.34, the calculated density is 1.300 g/cm.

On the basis of the systematic absences of *hkl*: $h + k/2n$, packing considerations, a statistical analysis of intensity distribution, and the successful solution and refinement of the structure, the space group was determined to be $C_{2/m}$ (no. 12). These data were collected at a temperature of 20 ± 1 °C using the $w-2j$ scan technique to a maximum $2j$ value of 50.1°. Omega scans of several intense reflections, made prior to data collection, had an average width at half-height of 0.31° with a take-off angle of 6.0°. Scans of $(1.78 + 0.30 \tan j)°$ were made at a speed of 8.0 deg/min (in θ). The weak reflections ($I < 10.0\sigma(I)$) were rescanned (maximum of five rescans), and the counts were accumulated to assure good counting statistics. Stationary background counts were recorded on each side of the reflection. The ratio of peak counting time to background counting time was 2:1. The diameter of the incident beam collimator was 1.0 mm, and the crystal to detector distance was 200.0 mm.

A total of 604 unique reflections were measured, and the final data: parameter ratio was 5.04 with $R = 0.036$, $R_w = 0.038$, and GOF = 1.19. For more details, see the supporting information.

Monomer−Dimer K_{eq} Determination for 2 and 5. 5 (2.2 mg) was dissolved in 0.50 mL of toluene-d_8 in a 5 mm NMR tube, and the ^{1}H NMR (400MHz) spectrum of the solution was recorded at 306.5, 332.0, and 364.5 K. The spectrometer probe temperature was measured using a previously calibrated ethylene glycol sample according to the chemical thermometer method.[37] All samples were allowed to equilibrate for at least 30 min at each temperature. To verify further that the azodioxide monomer:dimer ratio had reached equilibrium, NMR spectra were recorded at ~5 min intervals at a given temperature until relative signal intensities remained unchanged. The baseline-resolved 2H multiplet proton signals of dimer **5** (δ 1.20 ppm) and monomer **5m** (δ 1.05 ppm) were monitored at each temperature and their integrated intensities used to determine the monomer:dimer ratio. From these data, K_{eq} (eq 1) was calculated at 306.5, 332.0, and 364.5 K to be 0.00194, 0.0197, and 0.217 M, respectively. A plot of $1/T$ vs ln K_{eq} gave a best fit line ($r^2 = 1.00$) with slope −9069.1 and intercept 23.337, yielding $\Delta H° = 18$ kcal/mol and $\Delta S° = 46$ cal/mol deg for monomerization of **5** in toluene.

In the case of azodioxide **2**, 4.4 mg of solid **2** was dissolved in 0.50 mL of $CDCl_3$ and ^{1}H NMR (300 MHz) spectra were recorded at 25 °C periodically over 4 h. Time evolution of the spectra allows assignment of the peaks due to monomer **2m** and those due to dimer **2**. After 4 h in solution, an equilibrium mixture of **2m** and **2** existed and was analyzed as described above for **5** and **5m** mixtures. The result gave K_{eq} for **2**'s monomerization in $CDCl_3$ at 25 °C of 1.85 M.

Chemical Oxidation of *N,N'*-Dioxo-1,1'-azobis(norbornane) (5). Tris(*o,p*-dibromophenyl)aminium hexachloroantimonate[38] (25.7 mg, 0.024 mmol) was dissolved in 10 mL of CH_3CN. *N,N'*-dioxo-1,1'-azobis(norbornane) (**5**) (6.1 mg, 0.024 mmol) was added to the reaction flask at 25 °C under a nitrogen atmosphere while stirring rapidly. Stirring was continued for 1 h. The resultant solution was filtered to remove insoluble tris(*o,p*-dibromophenyl)amine and 1 mL of saturated aqueous $NaHCO_3$ was added, causing the blue solution to turn yellow. Solvent was evaporated at 25 °C *in vacuo*. The remaining aqueous paste was extracted with CH_2Cl_2 (3 × 5 mL). The CH_2Cl_2 extracts were combined, dried over anhydrous K_2CO_3, and evaporated *in vacuo*, leaving a pale yellow solid (11.4 mg). GC/MS and ^{1}H NMR analysis of the crude reaction mixture showed the major products to be starting azodioxide **5**, 1-norbornylacetamide (**10**) (assigned by comparison to authentic material prepared from acetylation of 1-norbomylamine), and tris(*o,p*-dibromophenyl)amine. The yield of **10** was quantitated relative to an added internal standard (1-adamantane−methanol) by coinjection using GC/MS response factors which were previously determined on our instrument using authentic samples. This analysis indicated that 0.012 mmol of 1-norbornylacetamide (**10**) (24% yield) formed in the reaction. Similar quantitation of the yield of **10** by ^{1}H NMR by

(34) Gassman, P. G.; Mansfield, K. T. *Org. Syntheses* **1973**, Collect. Vol. *5*, 96−101.

(35) Rieke, R. D.; Bales, S. E.; Hudnall, P. M.; Poindexter, G. S. *Org. Synth.* **1980**, *59*, 85−94.

(36) Golzke, V.; Groeger, F.; Oberlinner, A.; Rüchardt, C. *Nouv. J. Chim.* **1978**, *2*, 169−178.

(37) VanGeet, A. L. *Anal. Chem.* **1968**, *40*, 2227−2229.

(38) Schmidt, W.; Steckhan, E. *Chem. Ber.* **1980**, *113*, 577−585.

integration relative to added internal standard (nitromethane) confirmed the GC/MS results. Amide **10** observed in the reaction mixtures shows the following: MS (EI, *m/z*) 153 (M^+, 3), 124 (63), 82 (100); ^{1}H NMR ($CDCl_3$, 300 MHz) δ 1.29−1.40 (m, 2H), 1.60−1.81 (m, 8H), 1.92 (s, 3H), 2.14 (br s, 1H), 5.61 (br s, 1H).

Isolation of 11 from Chemical Oxidation of 5. ^{1}H NMR analysis of the crude reaction mixture from chemical oxidation of **5** by $Ar_3N^{\bullet+}$ (as above) showed the formation of a small amount of aromatic byproduct (~9%) which was isolated from the reaction mixture by preparative chromatography on silica gel using 2:1 hexane:methylene chloride elution ($R_f \sim 0.5$) to give a yellow oil. Further purification by Kugelrohr distillation (0.04 mm, 150 °C) gave a solid yellow material identified as bis(2,4-dibromophenyl)(2-bromo-4-nitrophenyl)amine (**11**): mp 223−225 °C; ^{1}H NMR (400 MHz, $CDCl_3$) δ 6.70 (d, 1H, J = 8.5 Hz), 6.73 (d, 1H, J = 8.5 Hz), 6.86 (d, 1H, J = 9.0 Hz), 7.36 (dd, 1H, J_1 = 8.5 Hz, J_2 = 2.2 Hz), 7.38 (dd, 1H, J_1 = 8.5 Hz, J_2 = 2.2 Hz), 7.74 (d, 1H, J = 2.2 Hz), 7.76 (d, 1H, J = 2.2 Hz), 8.05 (dd, 1H, J_1 = 9.0 Hz, J_2 = 2.6 Hz), 8.44 (d, 1H, J = 2.6 Hz); IR ($CHCl_3$, cm^{-1}) 3019, 1518, 1468, 1341, 1302; MS (EI, *m/z*) 683 (20), 524 (18), 399 (30), 239 (100), 199 (75), 120 (93). Anal. Calcd for $C_{18}H_9Br_5N_2O_2$: C, 31.57; H, 1.32; N, 4.15. Found: C, 31.43; H, 1.26; N, 4.15. CV analysis of **11** in 0.1 M TBAP/CH_3CN gave $E^{o\prime}$ = 1.68 V vs SCE.

Bulk Electrolysis of *N,N'*-Dioxo-1,1'-azobis(norbornane) (5). Controlled potential coulometry (CPC) was carried out using M-270 software from EG&G Princeton Applied Research. All chambers of the bulk electrolysis cell were filled with CH_3CN (0.1 M TBAP). A three-electrode system was used consisting of a working electrode (Pt foil, 3 × 5.5 cm) submerged into the large middle chamber of the cell, a reference electrode (Ag/Ag^+ in 0.1 M $AgNO_3$ in CH_3CN) placed in an adjoining chamber, and a counter electrode (coiled Pt wire) placed so as to have a buffer chamber between it and the working electrode chamber. The electrolyte solution in the working electrode chamber was deaerated prior to electrolysis and then cooled to −35 °C under N_2. *N,N'*-Dioxo-1,1'-azobis(norbornane) (**5**) (12.9 mg, 0.0516 mmol) dissolved in a minimal amount of CH_2Cl_2 was injected into the working electrode chamber after a pre-electrolysis time of 60 s, and the anode was held at a potential of 1.6 V vs the reference used during the electrolysis. Complete electrolysis of the substrate (one-electron oxidation/molecule) under these conditions took 10−15 min.

Spectroscopy of *N,N'*-Dioxo-1,1'-azobis(norbornane) Radical Cation ($5^{\bullet+}$). ESR. A red solution of $5^{\bullet+}$ (~2 mM) generated electrochemically in CH_3CN (0.1 M TBAP) at −35 °C was transferred cold via cannula to a 3 mm Pyrex tube (predried at 110 °C, purged with N_2, and sealed with a septum) cooled to below −35 °C. The tube was placed in the ESR cavity cooled to −35 °C and a five-line ESR spectrum (Figure 4) was observed.

UV−Vis. A red solution of $5^{\bullet+}$ (~2 mM) generated electrochemically as described above was transferred cold via cannula to a 1 cm Pyrex UV−vis cell (predried at 110 °C, purged with N_2, and cooled below −10 °C) equipped with a Teflon stopcock and a sidearm attached to a N_2 bubbler. The cell was transferred to a precooled (0 °C) UV−vis spectrometer sample compartment. The UV−vis spectrum from 190 to 820 nm was then recorded (see Figure 3).

Kinetics of *N,N'*-Dioxo-1,1'-azobis(norbornane) Radical Cation ($5^{\bullet+}$) Thermal Decay. A sample of $5^{\bullet+}$ prepared as described above for UV−vis spectroscopy was transferred to the UV−vis spectrometer cell holder (cooled to ~0 °C) and allowed to equilibrate thermally with stirring. The temperature of the solution was monitored by inserting a thermocouple into the cell. The UV−vis spectrometer was programmed to record spectra from 190 to 820 nm every 20 s for a total of 10 min. A final scan was taken after complete decomposition of the radical cation. The temperature of the solution over the reaction period was found to be 3 ± 1 °C. The decomposition rate of the radical cation was determined by monitoring the decrease in absorbance at 510 nm. First-order analysis of the data gave $k = 7.9 \times 10^{-3}$ s^{-1} with a relative standard deviation of 0.4% for the fit.

General Procedure for Chemical Oxidation of 1-Nitrosoadamantane (2m). A 30 mL three-necked round-bottomed flask containing a solution of **2m** (100 mg, 0.606 mmol) in CH_3CN (25 mL) was saturated with argon. One side-neck was connected to an Ar bubbler while the other side-neck was attached to a solid addition tube. Upon addition of a preweighed amount of oxidant, tris(*o,p*-dibromophenyl)-aminium hexachloroantimonate, the mixture was stirred until the reaction finished, as indicated by disappearance of the oxidant's color. The mixture was then transferred to a single-neck round-bottomed flask for removal of solvent under reduced pressure. The remaining crude solid was treated with 10% aqueous $NaHCO_3$ (~10 mL) and extracted with CH_2Cl_2 (4 × 10 mL). The combined CH_2Cl_2 layers were dried over anhydrous K_2CO_3, filtered, and concentrated under reduced pressure. Qualitative and quantitative analyses of crude products were performed by TLC and ^{1}H NMR. Nitromethane was used as internal standard in ^{1}H NMR measurements. The main crude products were *N*-1-adamantylacetamide (**13**), 1-adamantanol, and tris(2,4-dibromophenyl)amine (Ar_3N) which were identified by matching TLC and NMR responses to those of authentic samples. Results are given in Table 2.

Acknowledgment. We thank the NSF (CHE-9200144) for support of this research and Warren Craft for technical assistance. We acknowledge a Biomedical Research Support Grant (BRSG 2 S07 RR07201-11) for refurbishment of the Varian E-112 ESR spectrometer used in this work and an NSF instrument grant (CHE-8908065) for the funding of our X-ray diffraction facility.

Supporting Information Available: Details of X-ray structure determination with tables of atomic positional and thermal parameters (6 pages). This material is contained in many libraries on microfiche, immediately follows this article in the microfiche version of the journal, can be ordered from the ACS, and can be downloaded from the Internet; see any current masthead page for ordering information and Internet access instructions.

JA9436512